J Mol Model (2013) 19:119–130
DOI 10.1007/s00894-012-1528-7

ORIGINAL PAPER

Structure-based design of nitrogen-linked macrocyclic kinase inhibitors leading to the clinical candidate SB1317/TG02, a potent inhibitor of cyclin dependant kinases (CDKs), Janus kinase 2 (JAK2), and Fms-like tyrosine kinase-3 (FLT3)

Anders Poulsen · Anthony William · Stéphanie Blanchard · Harish Nagaraj · Meredith Williams · Haishan Wang · Angeline Lee · Eric Sun · Ee-Ling Teo · Evelyn Tan · Kee Chuan Goh · Brian Dymock

Received: 16 April 2012 / Accepted: 4 July 2012 / Published online: 22 July 2012

Abstract A high-throughput screen against Aurora A kinase revealed several promising submicromolar pyrimidine-aniline leads. The bioactive conformation found by docking these leads into the Aurora A ATP-binding site had a semicircular shape. Macrocycle formation was proposed to achieve novelty and selectivity via ring-closing metathesis of a diene precursor. The nature of the optimal linker and its size was directed by docking. In a kinase panel screen, selected macrocycles were active on other kinase targets, mainly FLT3, JAK2, and CDKs. These compounds then became leads in a CDK/FLT3/JAK2 inhibitor project. Macrocycles with a basic nitrogen in the linker form a salt bridge with Asp86 in CDK2 and Asp698 in FLT3. Interaction with this residue explains the observed selectivity. The Asp86 residue is conserved in most CDKs, resulting in potent pan-CDK inhibition by these compounds. Optimized macrocycles generally have good DMPK properties, and are efficacious in mouse models of cancer. Compound **5** (SB1317/TG02), a pan-CDK/FLT3/JAK2 inhibitor, was selected for preclinical development, and is now in phase 1 clinical trials.

Keywords SB1317 · Cyclin-dependent kinase · CDK2 · Fms-related tyrosine kinase · FLT3 · Kinase inhibitor · Janus kinase 2 · JAK2 · Structure-based design · Docking · Subtype selectivity · Bioactive conformation

A. Poulsen (✉) · A. William · S. Blanchard · H. Nagaraj · M. Williams · H. Wang · A. Lee · E. Sun · E.-L. Teo · E. Tan · K. C. Goh · B. Dymock
S*BIO Pte Ltd,
1 Science Park Road, #05–09 The Capricorn,
Singapore Science Park II,
Singapore 117 528, Singapore
e-mail: anders@colours.dk

Introduction

Over the last two decades, major advances have been made in the molecular understanding of the etiology of human cancers [1, 2]. One recurring theme has been the aberrant activation or mutation of protein kinases, important signaling mediators, with more than 20 kinases having been identified as being hyperactivated in diverse hematologic malignancies [2]. This paradigm has led to concerted efforts to develop small-molecule kinase inhibitors as novel anticancer therapeutics. The first targeted therapeutic agent of this type to be developed was imatinib, an inhibitor of the BCR-ABL fusion gene, which is the driver mutation found in leukemia patients harboring the Philadelphia chromosome. The unprecedented efficacy obtained with imatinib in chronic myelogenous leukemia (CML) has revolutionized the clinical management of this disease, establishing imatinib as the standard of care in newly diagnosed CML. This has intensified efforts to develop kinase-targeted therapies for other malignancies [1]. Examples of kinase inhibitors that have been approved since the development of imatinib include (i) second-generation BCR-ABL inhibitors like dasatinib and nilotinib, (ii) EGFR inhibitors like erlotinib, gefitinib, and lapatinib, and (iii) multi-kinase inhibitors like sunitinib and sorafenib. Many protein kinases hold great promise for the development of anticancer therapeutics, including three groups that will be described here: the Aurora kinases, the cyclin-dependent kinases, and Fms-like tyrosine kinase-3 (FLT3).

An introduction to the biological rationale for targeting Aurora kinases for oncology indications is available elsewhere [3]. Cyclin-dependent kinases (CDKs) are serine-

threonine kinases that play important roles in cell cycle control (CDK1, 2, 4, and 6), transcription initiation (CDK7 and 9), and neuronal function (CDK5) [4]. Aberrations in the cell cycle CDKs and their cyclin partners have been observed in various tumor types, including those of the breast, colon, liver, and brain [5]. It is believed that the pharmacological inhibition of CDK1, 2, 4, 6, and/or 9 may provide a new therapeutic option for cancer patients. In particular, the simultaneous inhibition of CDK1, 2, and 9 has recently been shown to result in enhanced apoptotic killing of lung cancer (H1299) and osteosarcoma cells (U2OS) compared with the inhibition of a single CDK alone [6]. Currently, several CDK inhibitors are in early-stage clinical trials, with the most advanced candidates being alvocidib (flavopiridol) and seliciclib (roscovitine), which have both entered phase II clinical testing.

Class III receptor tyrosine kinases (RTK), including c-Fms, c-Kit, FLT3, and platelet-derived growth factor receptors (PDGFRα and β), play important roles in the maintenance, growth, and development of hematopoietic and nonhematopoietic cells. Overexpression and activating mutations of these RTKs are known to be involved in the pathophysiology of diverse human cancers of both solid and hematological origin [2]. FLT3 mutations were first reported as an internal tandem duplication of the juxtamembrane domain-coding sequence; point mutations, deletions, and insertions surrounding the D835 coding sequence have since been found [7]. FLT3 mutations are the most frequent genetic alterations reported in AML, and are strongly associated with a poor prognosis. Currently, several FLT3 inhibitors are in clinical trials, with the most promising candidate being CEP701, which is in phase III testing.

We initiated an anticancer drug discovery program in search of small-molecule inhibitors of Aurora kinases. Our library of ~210,000 compounds was screened to identify inhibitors of the in vitro kinase activity of human recombinant Aurora A. Cell proliferation and histone biomarker assays were also used to select novel chemotypes for progression to lead optimization. Subsequent lead compounds were characterized more extensively for CDK2 and FLT3 activities.

A number of low nanomolar hits were obtained which shared the aniline-pyrimidine scaffold shown in Fig. 1. These chemotypes are known from the literature to be promiscuous kinase inhibitors, and have been heavily patented. The most potent inhibitors in this series were substituted with methoxy and hydroxy at the *meta* and *ortho* positions on the A ring, and had an additional substituent at the *beta* position on the B ring (Fig. 1). In order to create patentable matter, it was proposed to link R^1 and R^2 together to form a macrocycle which could be synthesized by ring-closing metathesis. This paper discusses the structure-based design of and explanations for the observed SAR which ultimately led to the clinical candidate SB1317/TG02 [8].

Computational methods

Conformational search, force fields, and solvation model

The molecules were built using Maestro 8.5.207 [9] or converted to 3D structures from the 2D structure using LigPrep version 2.5.207 [9]. Basic amines were protonated as in aqueous solution at physiological pH. The conformational space was searched using the Monte Carlo (MCMM) method [10] as implemented in MacroModel version 9.6.207 [9]. All heavy atoms and hydrogens on heteroatoms were included in the test for duplicate conformations. All rotatable single bonds were included in the conformational search, and all aliphatic rings were ring-opened and quaternary atoms were allowed to invert. Each search was continued until the global energy minima were found at least three times. The energy minimizations were carried out using the

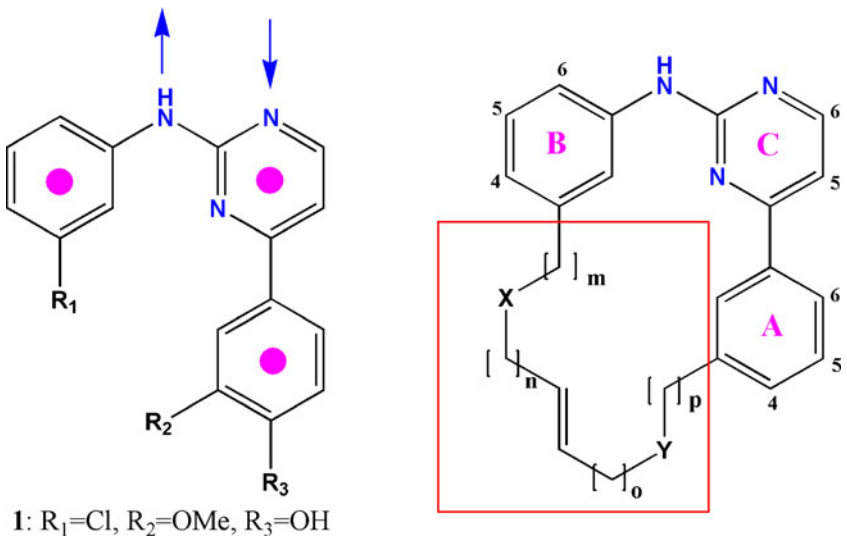

Fig. 1 *Left*: scaffold of the HTS leads. The *arrows* indicate hydrogen-bond interactions with the kinase hinge region. *Solid dots* indicate important hydrophobic interactions with the ATP-binding site. *Right*: structure of the proposed macrocycle. The three aromatic rings in the compounds discussed here will be referred to as the A, B, and C rings, respectively. The part of the macrocycle shown inside the *red box* will be referred to as the linker. Macrocycles compatible with our synthetic route and proposed binding mode could have *m*, *p*=0–2; *n*, *o*=1–3; and X, Y=NR, O, CONH, NHCO

truncated Newton conjugate gradient algorithm (TNCG) and the OPLS-2005 force field [11, 12] as implemented in MacroModel. The convergence was set to gradient with a threshold of 0.05, and the maximum number of iterations to 500. The conformational searches were done for aqueous solution using the generalized Born/solvent-accessible surface (GB/SA) continuum solvation model [13, 14]. A constant dielectric of 1.0 was used with an extended cutoff for van der Waals interactions of 8.0 Å, electrostatic interactions of 20 Å, and hydrogen bonds of 4 Å.

Docking

The Aurora A (PDB entry 1MQ4 [15]), Aurora B (PDB entry 2BFY [16]), and CDK2 (PDB entry 1AQ1 [17]) X-ray structures were downloaded from the Protein Data Bank (PDB, http://www.pdb.org). The protein structures were prepared using the protein preparation wizard in Maestro. Bond orders were assigned, hydrogens were added, and waters were deleted. Hydrogen bonds were assigned using exhaustive sampling of hydrogen bonds at neutral pH. Finally, the structures were minimized with Impref using OPLS-2005 with a convergence on heavy atoms of 0.3 Å. Grids were generated using Glide version 5.0.207 [9], following the standard procedure recommended by Schrödinger. The binding site was defined by the ligand and van der Waals radii were not scaled on the receptor. A hydrogen-bond constraint was included in the grid files. The backbone NH of the residue Ala213 (Aurora A), residue Ala273 (Aurora B), residue Cys694 (FLT3), or residue Leu83 (CDK2) must form a hydrogen bond to the ligand. This is the hydrogen-bond donor in the hinge region of the kinase to which the 1 position of the purine of ATP forms a hydrogen bond. The compounds were docked using Glide in standard precision mode with the settings "Sample nitrogen inversions," "Sample ring conformations," "Penalize nonplanar conformations of amide bonds," and a scaling factor for van der Waals radii of 0.8, with a partial charge cutoff set to 0.15. As Glide is unable to treat macrocyclic rings flexibly, a conformational search was performed on each compound, as previously described. The conformational ensemble was docked flexibly, i.e., only side chains were treated flexibly by Glide. The docked poses discussed in this paper were not necessarily the highest-scoring poses, but each was selected as the highest-scoring pose with a reasonable conformation and binding mode as judged by the modeler.

Protein modeling

The FLT3 (PDB entry 1RJB [18]) and FGFR2 (PDB entry 1OEC) X-ray structures were downloaded from the Protein Data Bank (PDB). The FLT3 X-ray structure is in the DFG-out conformation, which prevents our inhibitors from being docked into the ATP-binding site. A search of the PDB revealed that FGFR2 is the kinase domain structure with a DFG-in conformation with the highest homology to FLT3. The FGFR2 X-ray structure (PDB entry 1OEC) was superimposed onto FLT3 using the structure alignment tool in Maestro. Residues Asp829–Pro851 of FLT3 were manually modeled after the corresponding residues in the FGFR2 structure. The FLT3 model was subjected to 5000 steps of steepest-descent minimization using OPLS-2005 and GB/SA. The resulting hybrid X-ray/homology model FLT3 structure was prepared for docking as previously described, and residue Cys694 was used as constraint.

Calculation of the conformational energy penalty

The docked conformation was minimized with MacroModel using a flat-bottomed Cartesian constraint with a half width of 1.0 Å and a default restraining force constant of 100 kJ mol^{-1}. This allows the docked conformations to relax (adjust) to the OPLS-2005 force field. Without the relaxation, the energy calculated by OPLS-2005 would be meaningless. This relaxation does not change the conformation, as the RMS values between the docked and relaxed structures are <0.1 Å. The conformational energy penalty of the docked conformations was calculated by subtracting the internal (steric) energy of the preferred conformation in aqueous solution (i.e., the energy of the global energy minimum in solution excluding the hydration energy) from the calculated energy of the docked conformation. Since the conformational ensemble was represented by only the global energy minima, entropy effects have not been taken into account. For flexible molecules, this leads to underestimation of the energy penalty. A limit of 3 kcal mol^{-1} (12.6 kJ mol^{-1}) for acceptable energy penalties was imposed, as recommended by Boström et al. [19].

Calculation of physical properties

The 2D structures were converted to 3D using LigPrep with the -qik option. This option neutralizes the output structures, as is appropriate for QikProp input. Physical properties were calculated using QikProp version 3.1.207 [9] in standard mode.

DFT calculations

The program Jaguar version 7.5.207 [9] was used for hybrid B3LYP DFT energy minimization with a convergence criterion of 5×10^{-5} hartrees. The chosen basis set was 6-31G**. The PBF solvation model [20] was used with water as solvent, a dielectric constant of 80.37, and a density of 0.99823 g/ml. The accuracy level was set to "Accurate" and grid density was set to "Fine."

pK_a calculations were done using Jaguar's pK_a-prediction module. The accuracy level was set to "Accurate;" default parameters were used otherwise. The conformations used were the putative bioactive conformations obtained from docking, and were energy minimized using MacroModel.

In vitro kinase assays

The CDK2/cyclin A, FLT3, and JAK2 recombinant enzyme assays are described in [8], while the Aurora A and Aurora B assays are described in [3]. The analytical software Prism 4.0 (GraphPad Software Pte Ltd.) was used to generate IC_{50} values from the data.

Compound selection

The compounds described in this paper were selected due to interesting SAR properties that could be explained by structural interactions with one or more of the kinases Aurora A, CDK2, or FLT3. The CDK2, FLT3, and JAK2 data, as well as the synthesis and analytical data for compounds **2**, **5**, **7**–**8**, **11**–**12**, **15**, **17**–**21**, **28**, **30**, and **32**–**42** are described in [8]. The remaining compounds are reported for the first time in this article, and were synthesized as per the standard procedure described in [8].

Results and discussion

Binding-mode analysis and design of the macrocyclic linker

Docking of the leads obtained from the HTS analysis into the ATP-binding site of the active conformation of Aurora A revealed that the compounds were binding in a semicircular shape with the substituents at the *meta* positions on the A and B rings facing each other (Fig. 2). The aniline NH donor and the N acceptor at the 1 position on the pyrimidine ring both form hydrogen bonds to the backbone of Ala213 situated in the hinge region. The aromatic rings have hydrophobic contacts with Leu139, Ala160, Val147, Leu194, Leu263, and Ala273. The phenol may hydrogen bond to Lys162, the catalytic lysine, either through a water molecule or directly if the lysine moves 1 Å. This is not an unreasonable assumption, as the lysine side chain is very flexible and the experimental data show some variation in the position of the lysine side chain. The distance between the basic nitrogen of the Lys162 residue in a structural alignment of the Aurora A X-ray structures 1MQ4 and 3DAJ was 3.3 Å.

The proposed macrocycles have the generic structure shown in Fig. 1. *m*, *n*, *o*, and *p* have three options, and X and Y having four options. Since the double bond can be either *cis* or *trans*, the total number of possible linkers is 2592. It was expected that the major product of the ring-closing metathesis reaction would be the *trans* isomer. This has been confirmed, usually by ^{1}H NMR analysis, for the vast majority of compounds synthesized. To determine the optimal linker, 324 *trans* isomers with X=NH_2^+ were built. As Glide is unable to flexibly dock rings containing more than seven atoms, a conformational search was performed on each macrocycle. The obtained ensembles were then docked rigidly. The linkers that docked best had *m*=1, *n*=1–2, *o*=1–2, *p*=0, and Y=O or NH. Compound **2** (Fig. 3) is one of the compounds that docked best into Aurora A (Fig. 4). In addition to the interactions between the protein and inhibitor, the basic nitrogen of the macrocyclic linker may form a hydrogen bond to Thr217. Compound **5**, with X=NMe, *m*=*n*=1, *o*=2, *p*=0, and Y=O exhibited rather disappointing Aurora A activity (IC_{50}=1 μM), 100-fold less active than **1**. However, it was found that **5** potently inhibited cell proliferation, with GI_{50} values of 79 and 59 nM for the HCT-116 and HL60 cell lines, respectively [8]. Further investigations in a kinase panel screen revealed that **5** potently inhibited the cyclin-dependent kinases, particularly CDKs 2, 4, 7 and 9, as well as JAK2 and FLT3. The other members of the JAK family (JAK1, 3, and TYK2) were weakly inhibited. We were intrigued by this unusual kinase inhibitory profile. Consequently, our attention focused on the optimization of this series (Table 1).

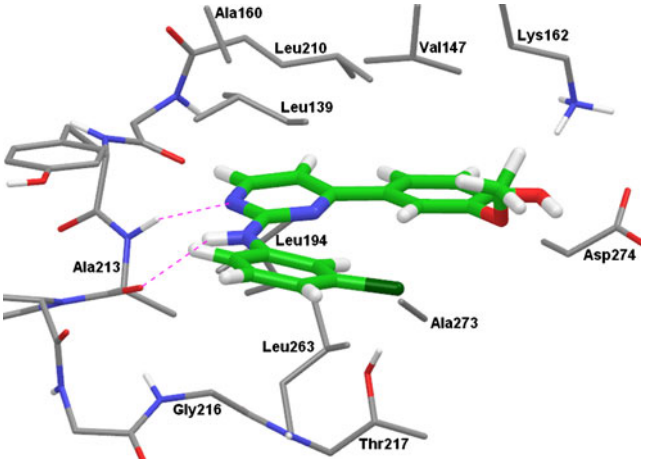

Fig. 2 The HTS lead compound **1** docked into the ATP-binding pocket of Aurora A. The protein is shown as *thin tubes with gray carbon atoms*. Only the side-chain heavy atoms are shown, except for hinge region residues, where the backbone is shown as well. Compound **1** is shown in *tube representation with green carbons*. Hydrogen bonds are shown as *magenta dashed lines*

Lead optimization studies and analysis of SAR

Compound **5** is a potent CDK2 and FLT3 inhibitor with activities of 13 and 56 nM, respectively. pK_a calculations

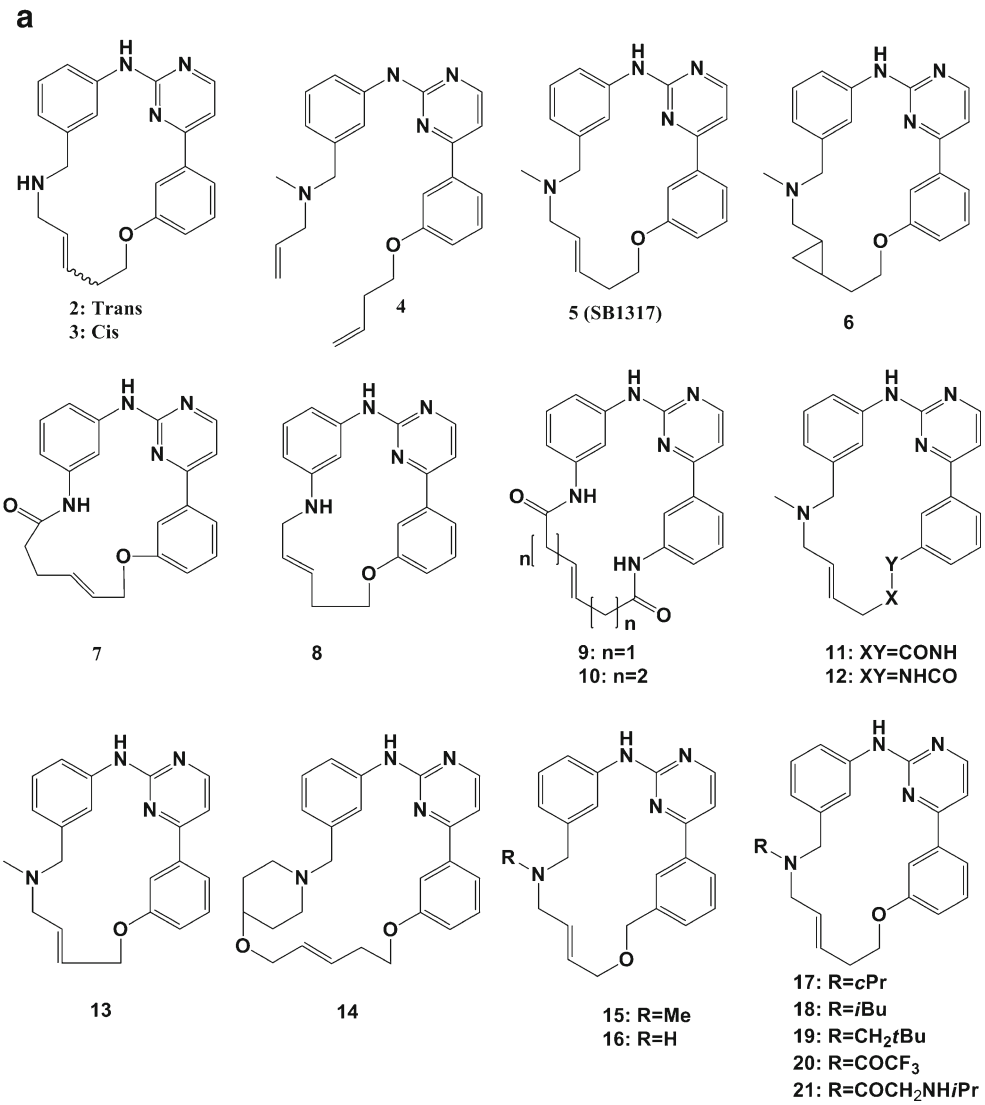

Fig. 3 Macrocycles synthesized for the CDK/FLT3 project. Biological data can be found in Table 1. All compounds except **3** are *trans* isomers

performed using the pK_a-prediction module of Jaguar suggest that the basic nitrogen linker is protonated at physiological pH, as the pK_a values of compounds **2** and **5** were found to be 9.2 and 8.8, respectively. While the basic nitrogen hydrogen bonds to Thr217 in Aurora A, the equivalent residues of CDK2 and FLT3 are both acids (Asp86/Asp698 in CDK2/FLT3). Figure 5a and b show compound **5** docked into CDK2 and FLT3, respectively. The basic nitrogen of **5** forms a salt bridge to both proteins. Note the similar positions of the aspartate residues of CDK2 and FLT3. This salt bridge may be one factor that explains the selectivity for CDK2/FLT3 over Aurora A.

Compound **4** is the substrate for the ring-closing metathesis reaction leading to **5**, and is much less active against the target kinases. Compound **4** docks into FLT3 and CDK2 in low-energy conformations, but the salt bridge between the basic nitrogen and the protein is absent. A higher-energy conformation is required for **4** to make the salt bridge. Compound **4** is also much more flexible than **5**, leading to a higher entropy penalty upon binding to the active site. Hence, there are probably two reasons for the much reduced inhibitory activity of **4**. Macrocyclization is essential in order to present the pharmacophore elements in the required conformation for binding to the protein by lowering the conformational energy penalty.

Synthesis of these macrocyclic compounds generally yields mixtures of *cis* and *trans* isomers which can be separated by chromatography or by selectively washing out the minor *cis* isomer with a suitable solvent. For example, comparing **2** and **3**, the *trans* isomer **2** is threefold more active against FLT3, whereas the CDK2 activities were similar. Compounds **2** and **3** were docked into FLT3 (not shown). Several *cis* and *trans* conformations docked well. The conformational energy was checked by solution-phase DFT B3LYP/6-31** calculations on the docked poses

Fig. 3 (continued)

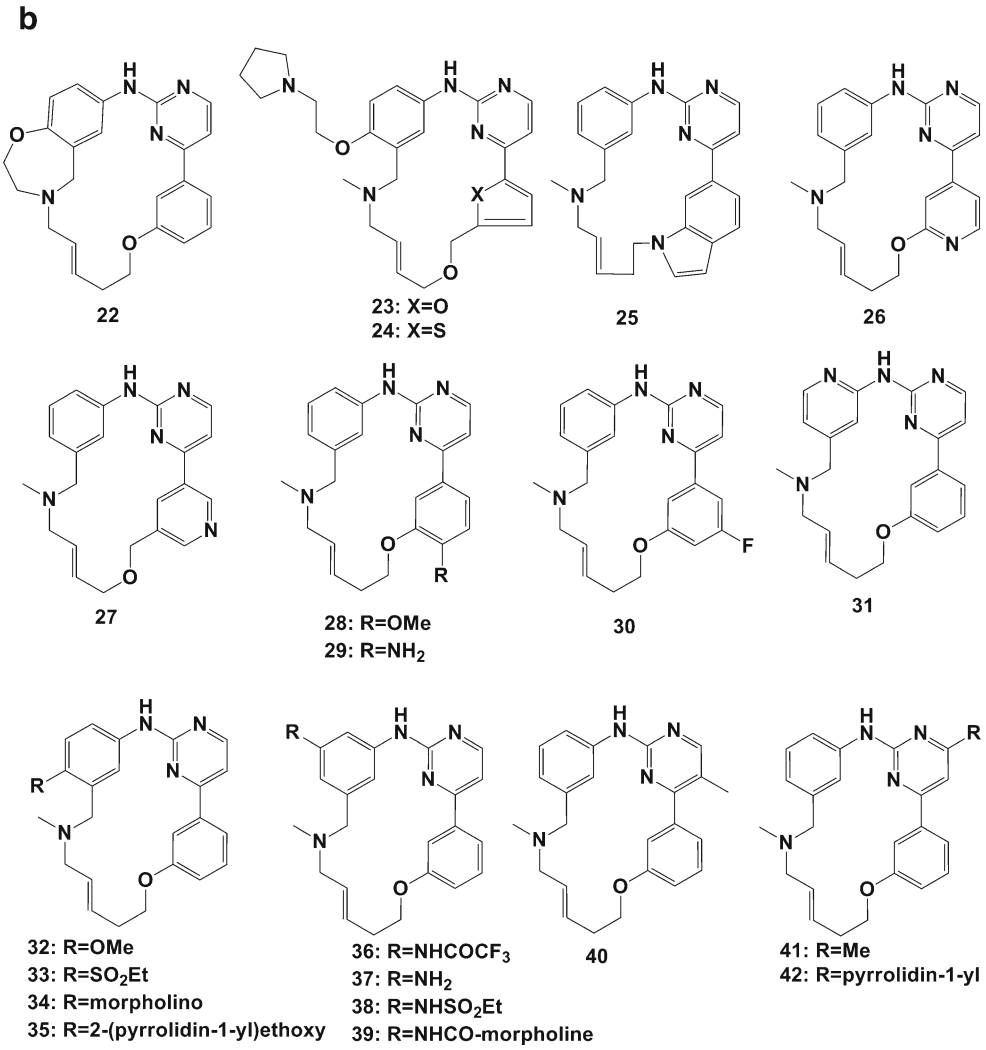

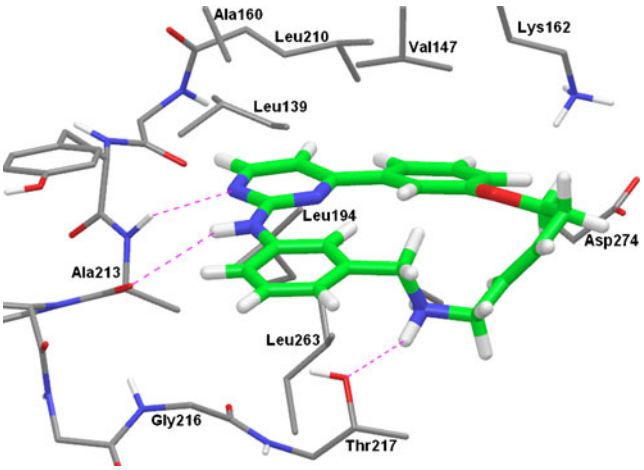

Fig. 4 Compound **2** docked into Aurora A. The aromatic ring system of the macrocycle forms the same interactions with the protein as **1**. In addition, the basic nitrogen of the linker may form a hydrogen bond with Thr217

and the global energy minima found by OPLS-2005. A high-scoring pose with a conformational energy within 1 kJ mol^{-1} of the global energy minima was found for both compounds of the *cis*/*trans* isomer pair. The solvation energy was found to be more negative for the *trans* isomer. Ignoring the entropy component, the conformational and solvation component of the free energy of binding cannot explain the observed difference in binding affinity between the *cis* and *trans* isomers. Therefore, we conclude that the *trans* isomer must have a more negative ligand–protein interaction energy than the *cis* isomer. See [19] for a discussion of the free energy of binding and its individual components. The activities of the *trans* isomers for other proteins (data not shown) were generally found to be more potent than those of the corresponding *cis* isomers. Figure 6 displays a superimposition of the docked poses of the *cis*/*trans* isomer pairs. Although the linkers of the isomeric pairs dock in approximately the

Table 1 Biological data for the compounds shown in Fig. 3. IC_{50} values (in μM) are expressed as the mean±standard deviation of at least two independent determinations

Compound	CDK2 IC_{50}	FLT3 IC_{50}	JAK2 IC_{50}	log*P*
2	0.021±0.012	0.11±0.03	0.15±0.08	3.8
3	0.014±0.004	0.32±0.10	0.17±0.01	3.7
4	2.1±0.5	0.47±0.10	0.72±0.03	5.9
5 (SB1317)	0.013±0.004	0.056±0.026	0.073±0.017	4.1
6	0.041±0.001	0.041±0.009	0.28±0.03	4.2
7	2.6±0.2	1.0±0.40	1.8±0.2	3.3
8	0.17±0.02	0.12±0.03	0.14±0.01	4.1
9	0.53±0.07	0.60±0.29	0.92±0.06	2.7
10	0.20±0.06	0.15±0.01	0.72±0.10	3.2
11	4.6±1.5	2.8±0.4	>10	3.0
12	>10	>10	>10	3.0
13	0.15±0.01	2.9±1.2	3.3±0.1	3.8
14	>10	>10	>10	4.4
15	0.66±0.19	0.21±0.02	1.7±0.1	3.7
16	0.17±0.02	0.47±0.02	1.0±0.1	3.4
17	0.036±0.017	0.042±0.006	0.090±0.02	4.6
18	0.2±0.1	0.19±0.01	1.5±0.1	5.0
19	>10	>10	>10	5.3
20	>10	>10	>10	4.4
21	0.53±0.09	0.14±0.06	0.12±0.01	3.6
22	0.095±0.001	0.080±0.024	0.13±0.01	3.8
23	1.55±0.49	0.12±0.06	0.33±0.050	3.5
24	0.71±0.42	0.012±0.003	0.09±0.01	3.9
25	0.077±0.001	0.093±0.005	1.6±0.07	4.8
26	0.022±0.002	0.31±0.01	0.26±0.01	3.8
27	0.42±0.09	4.8±0.1	>10	2.6
28	2.3±0.2	0.31±0.09	0.51±0.01	4.1
29	0.10±0.01	0.16±0.04	0.16±0.01	3.1
30	0.0089±0.0011	0.030±0.006	0.16±0.01	4.4
31	1.6±0.1	>10	>10	3.3
32	0.077±0.028	0.066±0.003	0.28±0.01	4.3
33	0.022±0.003	0.44±0.11	0.10±0.01	3.1
34	0.074±0.006	0.071±0.035	0.049±0.019	4.1
35	0.25±0.11	0.035±0.004	0.056±0.024	4.5
36	0.0079±0.0001	0.023±0.013	0.078±0.023	4.2
37	0.0065±0.0001	0.019±0.010	0.050±0.012	3.1
38	0.0080±0.0003	0.14±0.04	0.018±0.001	3.0
39	0.087±0.012	0.037±0.001	0.044±0.002	3.5
40	0.15±0.02	0.022±0.009	0.18±0.04	4.4
41	4.7±0.2	1.7±0.8	>10	4.5
42	>10	>10	>10	5.4

same area, there are some deviations, as indicated by the RMSD values from superimposition of the pair. This deviation results in a difference in the interaction with the protein. Generally, poses of *trans* isomers had more favorable van der Waals contact with the protein than *cis* isomers, as counted by the Glide scoring function.

Functionalization of the double bond was proposed as a way to introduce groups to increase the activity of the macrocycles. Cyclopropyl derivative **6** was docked into the binding sites of CDK2 (Fig. 7) and FLT3. The docked conformation of **6** is similar to that of the *trans* isomer **5**. The hydrogen of the cyclopropyl methylene points between

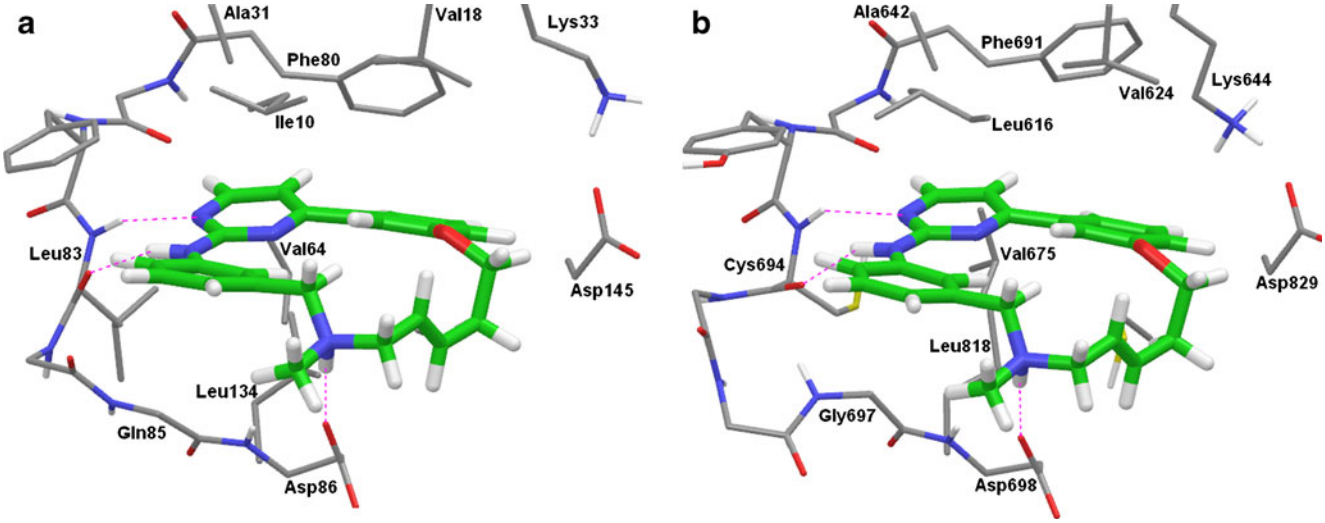

Fig. 5 **a** Compound **5** docked into CDK2. **b** Compound **5** docked into FLT3. Note that the basic nitrogen in the linker of **5** forms a salt bridge with Asp86 of CDK2 and Asp698 of FLT3. The displayed conformation of compound **5** docked well into both CDK2 and FLT3

the area where the phosphates of ATP bind and the exit from the binding site, so it was suggested as an attachment for a solubilizing group. Compound **6** is equipotent with **5** against FLT3 but threefold less potent on CDK2. In Fig. 7, favorable van der Waals interactions between **6** and CDK2 are shown with green dashed lines. Even though **6** is more lipophilic and has an extra methylene compared to **5**, it does not have better van der Waals interactions with CDK2. Log*P* values for the docked conformations are 4.1 and 4.2 for compound **5** and **6**, respectively. The conformational energy of the docked pose of **6** was found to be 3.5 kJ mol^{-1} less than that of **5**. However, this is within the uncertainty of the calculation. More favorable van der Waals interactions with the protein are probably the cause of the higher CDK2 affinity of **5**. There are four possible cyclopropyl isomers, which complicates the synthesis and characterization of the compounds. The synthesis of highly substituted cyclopropyl derivatives poses some challenges. For this reason, and the disappointing CDK2 activity of compound **6**, no further synthesis of cyclopropyl compounds was carried out.

It was initially thought that the basic nitrogen in the linker was also a metabolic liability, but stability studies in human and dog liver microsomes proved that the linker was metabolically stable, although this was not the case for rodent microsomes [8]. In a further study of the linker, several compounds with amide and aniline linkers were

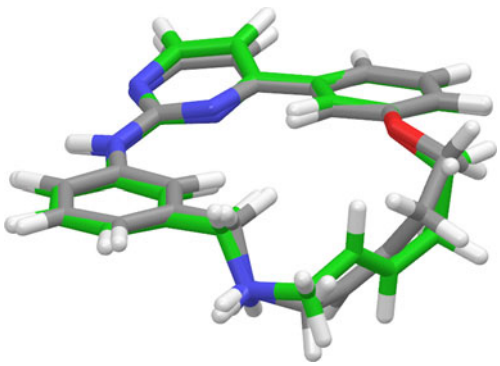

Fig. 6 Superimposition of the docked poses of the *cis*/*trans* isomers **2**–**3**. The *trans* isomers are shown as *thick tubes with green carbon atoms*, and the *cis* isomers as *thin tubes with gray carbon atoms*. The linkers of the *cis*/*trans* isomer pair occupy approximately the same area in the binding site. The RMSD from the superimposition of the docked poses over all heavy atoms is 0.49 Å. The maximum deviation is 1.53 Å

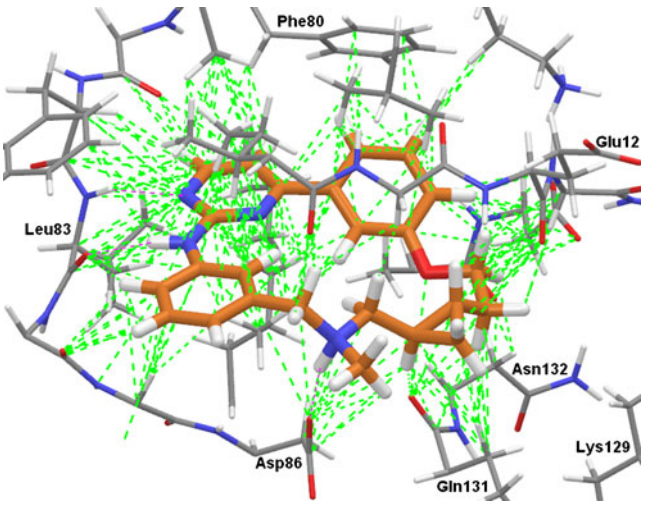

Fig. 7 Compound **6** docked into CDK2. CDK is shown as *thin tubes with gray carbons* and **6** is shown as *thick tubes with orange carbons*. Favorable van der Waals interactions between the compounds and CDK2 are shown as *green dashed lines*. The extra methylene in the cyclopropyl of compound **6** increases the number of favorable van der Waals interactions with the protein, but the conformational energy of the docked pose is higher than that of **5**. Note the edge-to-face interaction between the A ring and Phe80

synthesized. Docking indicated that the NH donor of the amides or aniline could form a hydrogen bond with Asp86 (Asp698) of CDK2 (FLT3). However, this hydrogen bond is a much weaker interaction than the salt bridge formed by **5**, and the probable cause of the 8–25-fold (3–6-fold) reduced CDK2 (FLT3) activities of these compounds (**7**–**10**). Compound **7** docked into CDK2 in a high-energy conformation, while the smaller **8** docked in a low-energy conformation and formed the hydrogen bond to Asp86. The same was found for the larger dual amide linked compounds **9**–**10**.

The optimal linker length for the macrocyclic ring was investigated. Docking into CDK2 indicated that the best linkers would have *m*, *n*=1, *o*=1–2, and *p*=0 (Fig. 1). The initial lead, **2**, satisfies this criteria, and compounds with different sized linkers such as compounds **8** and **13** are an order of magnitude less active than **5**. Compound **14** was predicted to be inactive, as it could not be docked in any reasonable conformation. Compounds **15** and **16** have the same linker size as compound **2**, but *o*, *p*=1 (benzylic, allylic ether), compared to *o*=2, *p*=0 (phenolic, homoallylic ether) for **2** and **5**. As the linker oxygen is conjugated with the A ring in **2**, the methylene connected to the oxygen is coplanar with the A ring in the global energy minima and the putative bioactive conformation. This is not the case for compounds **15** and **16**, so the difference in CDK2 activity may be attributed to this.

N substitution of the linker nitrogen was an attractive and synthetically straightforward opportunity, but docking revealed that there is only a small pocket in the CDK2 binding site for N substituents, with the largest aliphatic substituent that docked well being isobutyl. However, compound **18**, the isobutyl derivative of **2**, was an order of magnitude less potent against CDK2 and half as potent on FLT3. On the other hand, compound **17**, with a slightly smaller cyclopropane substituent, was equipotent with **2**, while compound **19**, with the larger 2,2-dimethyl propane substituent which did not dock well, was inactive against both CDK2 and FLT3. Docking indicated that there would be space to accommodate larger substituents if the linker nitrogen was flat, for example in the case of an amide nitrogen. However, if the linker nitrogen forms an amide with an N substituent, the nitrogen is neither an H-bond donor nor basic, and the salt bridge with Asp86 is lost. Compound **20**, the trifluoracetyl derivative of **2**, is inactive. Compound **21** is an amide derivative that incorporates a basic nitrogen; its FLT3 and JAK2 activities are similar to those of **2**, but its CDK2 activity was reduced by a factor of 20. It was proposed to form a ring between the N substituent and the B ring. Derivatives of **2** with five-, six-, and seven-membered rings docked well. For synthetic reasons, **22**, with a 1,4-oxazepane ring, was the only compound prepared. This compound was equipotent with **2** on FLT3, but four times less potent on CDK2.

Docking into CDK2 and FLT3 indicated that phenyl and pyrimidine were the optimal B and C rings, but low-energy conformations of various five-membered A-rings docked as well as or better than phenyl. Derivatives of **5** with five-membered heterocyclic A-rings were proposed, but only the synthetically accessible derivatives of the less active **15** were prepared. However, due to the choice of linker, these did not dock as well as compound **5**. Furan **23** was only slightly less active than **15** against CDK2, but JAK2 potency had increased fivefold. Note that **23** also has a solubilizing side chain that was designed for our JAK2-specific program (benzyl series) [21]. This increased JAK2 potency may be due to the change in the A ring or the basic side chain, but upon comparing **5** with its direct side chain-bearing analog **35**, CDK2 potency is reduced 20-fold for **35**. Therefore, the CDK2 activity of **15** is better than expected, suggesting that an A-ring heteroaryl group could be an attractive option. The slightly increased CDK2 activity of the thiophene **24**, as compared to **23**, may be due to the more lipophilic nature of this heterocycle.

In CDK2 (FLT3), the A ring is sandwiched between the hydrophobic residues Leu263 (Leu818), Ala273 (Cys828), and Val147 (Val624). The 4 position on the A ring points towards a hydrophilic area, with the distances to Lys33 (Lys644) and Asp145 (Asp829) being roughly 5 Å, so substitution at this position should be tolerated. Two strategies were available for modification of the A ring: carbon atoms could be added to increase hydrophobic contacts; or nitrogen atoms could be introduced in the 6 position to make hydrogen bonds to the flexible Lys33 (Lys644) and possibly with Asp145 (Asp829), mediated by a water molecule. Low-energy conformations of compounds with fused five- and six-membered A rings docked well and had more hydrophobic contacts with the proteins. However, **25** was synthesized and found to be two, five, and twenty times less potent against FLT3, CDK2, and JAK2, respectively, than **5**. Two pyridine derivatives of **5** were also synthesized. Compound **26** is roughly equipotent with **5** on CDK2, suggesting that any gain in electrostatic interactions with the protein is outweighed by the loss of hydrophobic interactions. The nitrogen of the A ring makes van der Waals contact with Ala273 in CDK2. In FLT3, the equivalent residue is the more hydrophobic Cys828, so the loss of hydrophobic contact with Cys828 may be the reason for the larger reduction in FLT3 activity. The A ring participates in an edge-to-face aromatic–aromatic interaction with the gatekeeper residue Phe80 (Phe691) (Fig. 7). The introduction of a nitrogen in the 5 position was expected to be detrimental to activity, as the negatively charged nitrogen should have a repulsive interaction with the π cloud of Phe80. Indeed, a 30-fold loss in CDK2 activity was observed with compound **27**.

Substitution of the 6 position on the A ring was realized with a hydrophobic methoxy substituent, leading to

compound **28**, which proved to be a rather poor CDK2 inhibitor (IC_{50} 2 μM). This compound docked in a low-energy conformation with more hydrophobic contacts than the unsubstituted analog **5**. However, the distance between the methoxy oxygen and the acid group of Asp145 is only 2.9 Å. This is a repulsive interaction that may explain the much reduced CDK2 activity. On the other hand, in the docked pose of aniline **29**, the NH_2 donor is within hydrogen-bonding distance of both Asp145 and Lys33. Lys33 is protonated and forms a salt bridge with Asp145. While the interaction of the aniline with Asp145 is attractive, the interaction with Lys33 is repulsive and the probable cause of the sevenfold-reduced CDK2 activity as compared to the unsubstituted **5**. The 5 position of the A ring points towards the *para* hydrogen of the gatekeeper Phe80. Docking indicated that fluorine was the only substituent small enough to be introduced at this position, and **30** proved to be slightly more potent on CDK2 than **5**.

Compound **31**, with a nitrogen at the 6 position on the B ring, was predicted to be less active due to the close repulsive interaction of the pyridine lone pair with the backbone carbonyl oxygen of Leu83. To challenge the modeling, the compound was synthesized and found to be 100 times less potent against CDK2 and to have IC_{50} values of >10 μM against FLT3 and JAK2.

Our attention then turned to B-ring substitutions at the 4 or 5 position, which point out of the binding site and are thus attractive opportunities for substitution. Docking of derivatives of **2** with a variety of groups at the 4 and 5 positions of the B ring indicated that there was room for groups that were directly attached or connected to a 2–3 atom linker. For ease of synthesis, the side chains were attached to the B ring using an oxygen, nitrogen, or sulfur atom. The 4-methoxy **32** was equipotent against FLT3 but five times less active for CDK2 compared to **5**. Ethyl sulfone **33** was roughly equipotent on CDK2, but was eightfold lower in FLT3 activity than **5**. Compound **35** with a pyrrolidinylethoxy group was slightly more potent on FLT3 but was 20-fold lower in CDK2 activity. Figure 8 (left) displays **33** docked into CDK2. There is just enough space for the substituent, as the ethylsulfonyl is in a low-energy out-of-plane conformation and the sulfone may form a hydrogen bond to Lys89. This conformation of **33** could not be docked into FLT3 without clashing with the protein. Figure 8 (right) displays **35** docked into FLT3. The pyrrolidinylethoxy side chain is in a low-energy in-plane conformation pointing straight out of the binding site. The ethanol linker binds above Asn701, while the pyrrolidine interacts with the protein surface. The interaction of the side chain with the surface of FLT3 is not particularly favorable, and the potency is only slightly increased compared to that of **5**. No low-energy conformations of **35** could be docked into CDK2 without clashing with the protein. The 4 position could accommodate short, bulky, directly attached substituents like the morpholino of **34**, which showed similar activities to those of **32**. The introduction of substituents at the 4 position changes the conformation of the macrocyclic linker slightly. If the 4-substituent is attached by an oxygen atom there is an internal electrostatic interaction with the basic nitrogen in the global energy minima. This may also contribute to the reduced CDK2 activities of compounds **32** and **35**. Compounds with a basic nitrogen in the macrocyclic

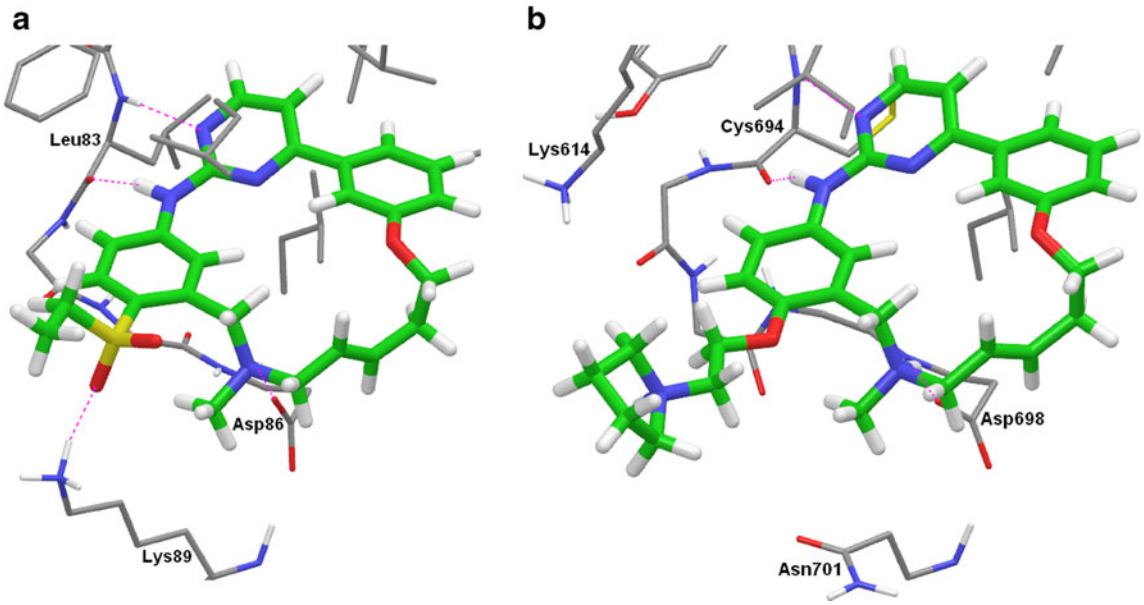

Fig. 8 **a** Compound **33** docked into CDK2. The sulfone forms an additional hydrogen bond with Lys89. **b** Compound **35** docked into FLT3. The pyrrolidine side chain is in a low-energy conformation and points straight out of the binding site. This conformation is not possible for the side chain when bound to CDK2

linker are already quite soluble and do not need the additional solubilizing group. Furthermore, since there was no potency advantage over **5**, this series was not progressed further.

The 5 position on the B ring points towards the backbone amide oxygen of His84 in CDK2 and Cys695 in FLT3. Docking indicated that an extra hydrogen bond could be formed with both proteins if the 5 position were substituted for an NH donor. Figure 9 displays trifluoroacetamide **36** docked into CDK2. The amide NH of **36** forms a hydrogen bond with His84 while the trifluoroacetyl side chain does not form any favorable interactions with the protein, as it points towards the solvent. Compound **36** is slightly more potent on both CDK2 and FLT3 than **5**. As **37** is equipotent with aniline **36**, it is apparent that only the hydrogen-bond donor contributes to the increased activity. It was hypothesized that a sulfonamide at the 5 position on the B ring could form an additional weak hydrogen bond with the flexible surface residue Lys89 of CDK2 (compare with Fig. 8a). However **38**, incorporating a sulfonamide, is equipotent with compounds **36** and **37** against CDK2, and ten times less active on FLT3. Compound **39**, bearing a morpholine-urea substituent, is two and fourteen times less potent than **37** against FLT3 and CDK2, respectively. Docking into FLT3 indicates that there is space for this substituent, while the morpholine clashes with Arg297 in CDK2.

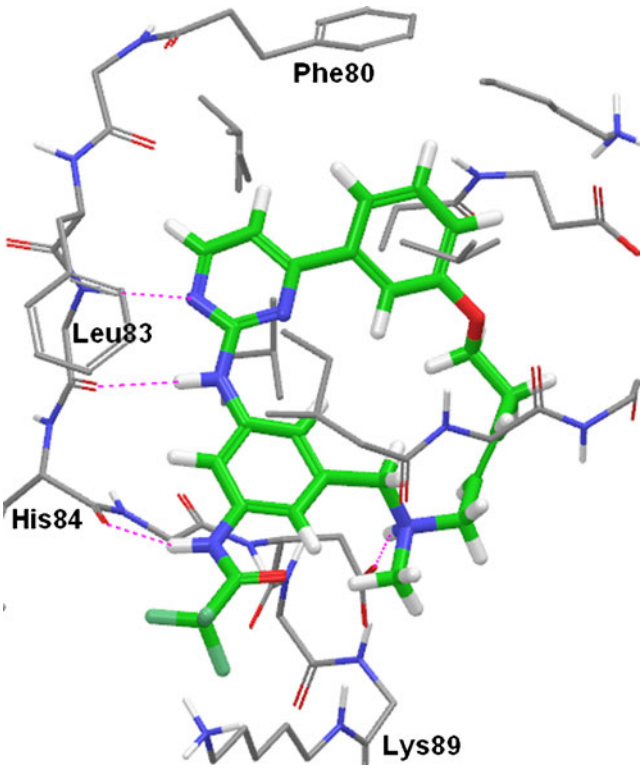

Fig. 9 Compound **36** docked into CDK2. The amide NH at the 5 position on the B ring forms an additional hydrogen bond to the carbonyl oxygen of His84 in the protein backbone at the end of the kinase hinge region

Docking into FLT3 revealed that there is space for small substituents like Cl, Br, and Me at the 5 position of the C ring. The 5 position points towards the gatekeeper residue Phe80 in CDK2 and Phe691 in FLT3. Low-energy conformations of **40** docked well into both CDK2 and FLT3 with increased hydrophobic contact as compared to **5** without the 5-Me substituent. However when 5-Cl-, 5-Br-, or 5-Me-substituted compounds are docked into CDK2, the poses are shifted slightly along the hinge axis away from the gatekeeper compared to unsubstituted compounds. This shift is not observed for FLT3 poses. Compound **40** is twice as potent on FLT3 as **5**, but only one-tenth as potent on CDK2. Figure 10 shows a superimposition of CDK2 and FLT3. It is apparent that there is more space for substituents in front of the gatekeeper residue in FLT3 than in CDK2.

The 6 position on the C ring points towards the amide oxygen of the backbone of Ala81 in CDK2 and Glu692 in FLT3. The distance between H6 on the C ring and the oxygen is 2.3 Å. This is roughly the same distance as between the hydrogen donor and acceptor in a hydrogen bond, so there is clearly no space for substituents at this position (Fig. 10). As the hydrogen atoms in aromatic rings have a positive partial charge, some authors have speculated that this is indeed a real hydrogen bond, although the interaction energy is lower than hydrogen bonds between two heteroatoms [22]. To challenge the modeling, compounds **41** and **42** with methyl and pyrrolidinyl, respectively, were synthesized and proved to have much reduced activities.

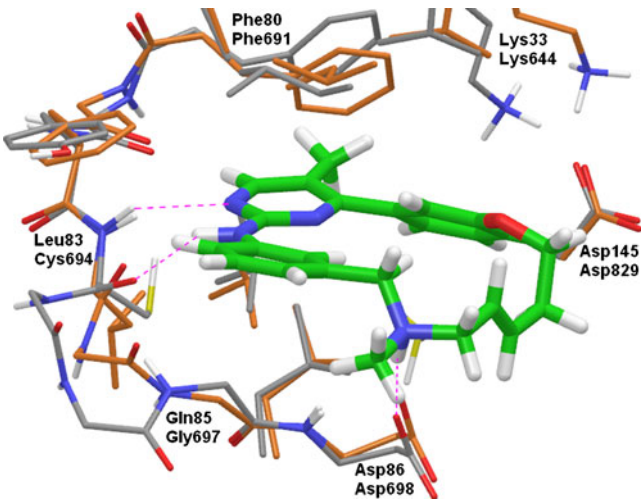

Fig. 10 Compound **40** docked into FLT3. FLT3 is shown as *thin tubes with gray carbons*, while **40** is shown as *thick tubes with green carbons*. CDK2 (*thin tubes with orange carbons*) has been superimposed onto FLT3 by structural alignment. There is more space in front of the gatekeeper in FLT3 than in CDK2. The methyl substituent prevents the A ring from having edge-to-face interactions with Phe80 in CDK2. Notice that, compared to CDK2, there is an insertion in FLT3 between Cys694 and Gly697. However, the crucial residues for the salt bridge and the hydrogen-bond interactions are at the same positions in the two proteins

Conclusions

An Aurora A HTS hit was modified by macrocyclisation via ring-closing metathesis to achieve novel small-molecule macrocycles. Docking revealed that an eight-atom linker incorporating two heteroatoms and a double bond was optimal. The enzyme-inhibitory activities of the resulting compounds were in the high nanomolar range, but were 100-fold less active than the HTS lead against Aurora A. Profiling the macrocycles in a kinase panel revealed them to be potent CDK/FLT3 inhibitors. Aurora A and CDK2/FLT3 differ in the residue that interacts with the basic amine in the macrocyclic linker, which is Thr217 in Aurora A, and may form a hydrogen bond to the macrocycle. The equivalent residue Asp86/Asp698 in CDK2/FLT3 may form a salt bridge to the basic amine in the macrocyclic linker, explaining the difference in selectivity over Aurora A.

The optimized compounds have low-nanomolar pan-CDK, FLT3, and JAK2 kinase inhibitory activities. The vast majority of the SAR could be explained by modeling studies. The selected compounds have good DMPK properties and are active in cell-based and mouse models of cancer [8]. Due to the basic nitrogen in the macrocyclic linker, a polar solubilizing side chain is not needed to improve solubility. During lead optimization, it was possible to improve in vitro potency against kinase activities, but this generally came at a cost to either the ADMET properties or selectivity [8]. Compound **5**, a pan-CDK/FLT3/JAK2 inhibitor with balanced potency and ADMET properties, has entered phase 1 clinical development for advanced/refractory hematologic malignancies and multiple myeloma as SB1317/TG02 [8].

References

1. Chalandon Y, Schwaller J (2005) Targeting mutated protein tyrosine kinases and their signaling pathways in hematologic malignancies. Haematologica 90:949–968
2. Hannah AL (2005) Kinases as drug discovery targets in hematologic malignancies. Curr Mol Med 5:625–642
3. Poulsen A, William AD, Lee A, Blanchard S, Teo EL, Deng WP, Tu N, Tan E, Sun ET, Goh KL, Ong WC, Ng CP, Goh KC, Bonday Z (2008) Structure-based design of Aurora A & B inhibitors. J Comput Aided Mol Des 22:897–906
4. Knockaert M, Greengard P, Meijer L (2002) Pharmacological inhibitors of cyclin-dependent kinases. Trends Pharmacol Sci 23:417–425
5. Shapiro GI (2006) Cyclin-dependent kinase pathways as targets for cancer treatment. J Clin Oncol 24:1770–1783
6. Cai D, Latham VM Jr, Zhang X, Shapiro GI (2006) Combined depletion of cell cycle and transcriptional cyclin-dependent kinase activities induces apoptosis in cancer cells. Cancer Res 66:9270–9280
7. Parcells BW, Ikeda AK, Simms-Waldrip T, Moore TB, Sakamoto KM (2006) FMS-like tyrosine kinase 3 in normal hematopoiesis and acute myeloid leukemia. Stem Cells 24:1174–1184
8. William AD, Lee A, Goh KC, Blanchard S, Poulsen A, Teo EL, Nagaraj H, Lee C, Wang H, Williams M, Sun ET, Hu C, Jayaraman R, Pasha MK, Ethirajulu K, Wood JM, Dymock BW (2012) Discovery of kinase spectrum selective macrocycles (16E)-14-methyl-20-oxa-5,7,14,26-tetraaza-tetracyclo[19.3.1.1(2,6).1(2,12)heptacosa-1(25),2(26),3,5,8(27),9,11,16,21,23-decaene (SB1317/TG02), a potent inhibitor of cyclin-dependent kinases (CDKs), Janus kinase 2 (JAK2) and Fms-like tyrosine kinase-3 (FLT3) for the treatment of cancer. J Med Chem 55:169–196
9. Schrödinger, LLC (2012) Maestro, LigPrep, MacroModel, Glide, QikProp & Jaguar. Schrödinger, LLC, New York. http://www.schrodinger.com
10. Chang G, Guida WC, Still WC (1989) An internal-coordinate Monte Carlo method for searching conformational space. J Am Chem Soc 111:4379–4386
11. Jorgensen WL, Maxwell DS, Tirado-Rives J (1996) Development and testing of the OPLS all-atom force field on conformational energetics and properties of organic liquids. J Am Chem Soc 118:11225–11236
12. Kaminski GA, Friesner RA, Tirado-Rives J, Jorgensen WL (2001) Evaluation and reparametrization of the OPLS-AA force field for proteins via comparison with accurate quantum chemical calculations on peptides. J Phys Chem B 105:6474–6487
13. Hasel WH, Hendrickson TF, Still WC (1988) A rapid approximation to the solvent accessible surface areas of atoms. Tetrahedron Comput Method 1:103–116
14. Still WC, Tempczyk A, Hawley RC, Hendrickson T (1990) Semianalytical treatment of solvation for molecular mechanics and dynamics. J Am Chem Soc 112:6127–6129
15. Nowakowski J, Cronin CN, McRee DE, Knuth MW, Nelson CG, Pavletich NP et al (2002) Structures of the cancer-related Aurora-A, FAK, and EphA2 protein kinases from nanovolume crystallography. Structure 10:1659–1667
16. Sessa F, Mapelli M, Ciferri C, Tarricone C, Areces LB, Schneider TR et al (2005) Mechanism of Aurora B activation by INCENP and inhibition by hesperadin. Mol Cell 18:379–391
17. Lawrie AM, Noble ME, Tunnah P, Brown NR, Johnson LN, Endicott JA (1997) Protein kinase inhibition by staurosporine revealed in details of the molecular interaction with CDK2. Nat Struct Biol 4:796–801
18. Griffith J, Black J, Faerman C, Swenson L, Wynn M, Lu F, Lippke J, Saxena K (2004) The structural basis for autoinhibition of FLT3 by the juxtamembrane domain. Mol Cell 13:169–178
19. Bostrom J, Norrby PO, Liljefors T (1998) Conformational energy penalties of protein-bound ligands. J Comput Aided Mol Des 12:383–396
20. Tannor DJ, Marten B, Murphy R, Friesner RA, Sitkoff D, Nicholls A, Ringnalda M, Goddard WA, Honig B (1994) Accurate first principles calculation of molecular charge distributions and solvation energies from ab initio quantum mechanics and continuum dielectric theory. J Am Chem Soc 116:11875–11882
21. William AD, Lee A, Goh KC, Blanchard S, Poulsen A, Teo EL, Nagaraj H, Tan E, Chen D, Williams M, Sun ET, Goh KC, Ong WC, Goh SK, Hart S, Jayaraman R, Pasha MK, Ethirajulu K, Wood JM, Dymock BW (2012) Discovery of the macrocycle 11-(2-pyrrolidin-1-yl-ethoxy)-14,19-dioxa-5,7,26-triaza-tetracyclo[19.3.1.1(2,6).1(8,12)]heptacosa-1(25),2(26),3,5,8,10,12(27),16,21,23-decaene (SB1518), a potent Janus kinase 2/Fms-like tyrosine kinase-3 (JAK2/FLT3) inhibitor for the treatment of myelofibrosis and lymphoma. J Med Chem 54:4638–4658
22. Desiraju GR, Steiner T (1990) The weak hydrogen bond. In: Structural chemistry and biology. Oxford University Press, Oxford, p 507